ARCHIVES OF ELECTRICAL ENGINEERING VOL. X(Y), pp. 1-20 (2026)

This paper has been accepted for publication in the AEE journal. This is the version, which has not been fully edited and content may change prior to final publication. Citation information: DOI 10.24425/aee.2026.1692

Design of a robust controller with guaranteed H∞ criteria for a servo system considering summative and polytopic uncertainty

Bing Ge, Ce Cao*

Changchun Institute of Optics, Fine Mechanics and Physics, Chinese Academy of Sciences Changchun 130000, Jilin, China

email: 15504307098@163.com

Abstract: This paper addresses the challenge of robustness against model uncertainties as well as simplicity in controller design for position control in servo systems. More specifically, in this paper, during the modeling of a permanent magnet synchronous motor for a servo system, uncertainties of the model are considered and are introduced as a summative term in its state space equation. But to increase the controller robustness, in addition to this cumulative uncertainty term, a polytopic uncertainty is also considered in the model design for the system state matrix. The system becomes fully robust to uncertainties after modeling. A state feedback controller is then designed based on this model, ensuring that the H∞ performance criterion is satisfied. In this way, and by satisfying the H∞ condition, the controller becomes robust against uncertainties accumulated by the model. On the other hand, the considered polytopic uncertainties also create a resistance to the uncertainties of the system's transient matrix. The advantage of the method presented in this article is that it has a very simple structure and its design is very simple. It also has a low computational burden and, despite its simplicity, has very good resistance to uncertainties. In addition, the proposed method also eliminates the chattering problem that exists in the sliding mode control family. To examine the performance of the proposed method, a series of experiments was conducted in the laboratory, and the results confirmed the effectiveness of this method in the cases mentioned above.

Keywords: H∞ criteria, polytopic uncertainty, servo system, state feedback controller, summative uncertainty

1. Introduction

For servo systems based on permanent magnet synchronous motors (PMSMs), accuracy in rotor angle control is essential for industrial drives, robotics, and CNC machines. Numerous control strategies have been developed to enable precision position accuracy, rapid transients, robust performance under disturbance, and efficiency over time throughout the last several decades. In a way, the literature has revealed a natural classification of strategies based on levels of abstraction, starting with traditional linear controllers, and finishing with today's nonlinear

This paper has been accepted for publication in the AEE journal. This is the version, which has not been fully edited and content may change prior to final publication. Citation information: DOI 10.24425/aee.2026.1692

and intelligent strategies, each corresponding to the nonlinearity and fast dynamics of PMSMs themselves [1], [2].

Initial methods for controlling the angle for PMSMs often use a linear or linear approximation: just as PID (proportional-integral-derivative) controllers [3], often with added feedforward terms from the motor model, form the basis for many industrial servo systems [4]. In these schemes, the angle error is the difference between the commanded rotor angle and the actual measured angle. The error is passed through a feedback loop to adjust the current components that provide torque. Linear-quadratic regulators (LQRs) [5] and model predictive control (MPC) [6], [7], where the plant is modeled, also have systematic design routes that make a tradeoff between tracking performance and control effort that minimizes a quadratic cost function. There are advantages of analytic tractability and ease of implementation, but they all happily assume sufficiently linear responses and enough model accuracy, which can be severely challenged by parameters that can vary, nonlinear friction, and magnetic saturation [8]. A substantial body of work focuses on leveraging accurate motor models and state observers to estimate unmeasured states and to compensate for disturbances. Extended Kalman filters (EKFs) [9] and sliding mode observers (SMOs) [10] are used most often to estimate rotor speed, rotor position, and flux linkages in the presence of measurement noise. Observers provide robust estimates of the mechanical angle even in sensorless configurations, where resolver or encoder signals may be corrupted, when the rotor angle is the primary controlled variable. Using proportional-integral observers or disturbance observers (DOBs) [11] allows for the mitigation of model mismatch and disturbance due to load torque disturbances. Model-based controllers may be combined with backstepping or input–output linearization to manage the nonlinear stator currents to torque relationship, with better stability margins and less tracking error at reasonable control effort levels [12]. The nonlinear nature of PMSMs—the torque–angle behavior and the cross-coupling between the d- and q-axis dynamics—encourages nonlinear control methods. For example, backstepping methods [13] formulate a cascaded virtual control law for the transformed system that incorporates Lyapunov stability, with a direct connection to angular errors. Input-output feedback linearization [14] considers the nonlinear plant to get a linearized input-output map so that linear controllers can be utilized on the transformed system. Passivity-based controls use energy functions to ensure stability, even in the presence of uncertain payloads and frictional disturbances. Although nonlinear control methods usually offer better transient performance and wider operating quadrants, care must be taken to avoid overdesigning for unknowns or producing solutions that are computationally infeasible [15]. H∞ and μ-synthesis robust control [16] formulations are used to provide performance guarantees in the case of motor parameter drift. Motor parameter drifts may be due to temperature effects, aging characteristics, or manufacturing tolerances. For example, the design of robust control formulations explicitly considers structured uncertainties in the motor's inductance values, back-EMF constants [17], and resistance characteristics of the motor's windings, thus permitting guaranteed performance bounds in response to perturbations. In the case of adaptive control schemes, increasingly sophisticated schemes are designed to change controller gains (and/or reference models) to adapt to slowly varying parameters. In the case of angle control, this adaptation may occur in rotor

This paper has been accepted for publication in the AEE journal. This is the version, which has not been fully edited and content may change prior to final publication. Citation information: DOI 10.24425/aee.2026.1692

inertia terms, load torque terms, or back-EMF constants, which allows for the mitigation of accumulated error due to changes in mechanical conditions. These adaptive schemes have the benefit of being easy to implement in servo applications that have variable payloads and possibly complex friction profiles, although convergence and stability results frequently depend on persistent excitation and well-designed adaptation laws [18]. Sliding mode control (SMC) [19] has proven itself as an effective method for output angle (position) control of PMSMs used in server systems, where performance on angle is paramount, fast, and disturbance-tolerant. Earlier research has used concepts of high-order SMC and equivalent control to counter the motor nonlinearities, parametric uncertainty, and measurement noise, which resulted in better disturbance rejection and ultimately finite-time convergence. The literature shares the concept of a sliding surface designed around rotor position error and derivatives using a robust control law that guarantees convergence in spite of friction, load changes, and electrical parameter variation [20]. Discontinuous control actions offer robustness, but there are chattering concerns; thus, authors have presented boundary-layer formulations, adaptive switching gains, or continuous approximations (such as sigmoid or saturation functions) to trade off robustness for actuator wear and acoustic noise, without opening the feedback loop. Model-based adaptations are emerging designs that account for the PMSM's nonlinear electromagnetic dynamics, such as in flux-weakening or saliency-aware SMC, to permit accurate torque and speed tracking over a wide speed range, suitable for server cooling or precision drive applications. Hybrid methods include proportional-derivative (PD) and backstepping layers added to SMC to improve steady-state targeting and limit the rate of switching. Newer methodologies demonstrate the use of adaptive or recursive learning to estimate uncertain inertia, friction, and time-varying load torques online, providing robustness to these uncertainties without relying heavily on precise knowledge of the motor parameters. SMC's strong robustness to uncertainties and disturbances makes it an attractive option for PMSM angle control in the server context, and it is encouraging to see literature on mere practical adoptability and minimizing chattering [21]. A large part of the literature studies sensorless PMSM control, which uses electrical measurements to estimate rotor angle [22], instead of having direct angular sensors. Beginning with the estimation of rotor position/speed, sensorless designs often incorporate estimators into control loops to keep angle tracking accurate. Models of the motor yield observers [23], such as a sliding-mode observer or high-gain observer, that provide robustness to measurement noise and mechanical disturbance. Regardless of the observer-based estimation, or, typically, the angle control problem in sensorless contexts requires consideration of position/speed estimates, particularly during low-speed and standstill conditions, where the back-EMF observations diminish considerably. A hybrid solution to tracking the angle across the speed band is achieved through estimation combined with periodic sensor readings. Recent developments include optimization-based methods and data-driven approaches to improve angle control performance [24]. MPC for the case of PMSMs is an example of computing the optimal torque commands from solving a finite-horizon optimization problem respecting actuator saturation and torque limits; MPC also provides a method to smoothly track setpoints while explicitly respecting performance and energy objectives [25]. Reinforcement learning [26] and neural-network-based controllers [27]

This paper has been accepted for publication in the AEE journal. This is the version, which has not been fully edited and content may change prior to final publication. Citation information: DOI 10.24425/aee.2026.1692

have potential for adapting to nonlinearities and unknown disturbances and possibly even reducing dependency on accurate offline modeling. These methods aim to provide high-quality positioning with strong generalization robustness, but they require large amounts of training data and computational resources, and safety considerations must be addressed before deploying them in real-time industrial applications [28].

In addition to academic control methodologies, manufacturers of CNC machine tools and industrial motion control systems have developed and documented practical solutions for managing uncertainties in servo-driven axes. Technical publications from companies such as Fanuc, Siemens, and Bosch Rexroth emphasize real-time compensation techniques for friction, load inertia variations, and thermal effects—key sources of summative and polytopic uncertainty in production environments. For instance, Siemens' drive-internal advanced position control (APC) functions and Fanuc's servo tuning guides describe gain scheduling and adaptive filtering methods that maintain positioning accuracy under changing operating conditions without requiring complex model reformulation. Similarly, Yaskawa's motion control handbooks discuss robustness improvements via disturbance observers and vibration suppression loops, which align conceptually with the H∞ criteria used in this work. These manufacturer-driven approaches highlight the industrial relevance of achieving robust performance with low computational overhead, reinforcing the motivation for the simple yet effective controller structure proposed in this paper.

This work addresses the challenge of attaining robustness to model uncertainties while minimizing complex controller designs for position control of a servo system. More specifically, when modeling a permanent magnet synchronous motor for a servo application, model uncertainties are included as a summative term in the state-space model formulation. To improve robustness, some of the uncertainty is also included as polytopic uncertainty in the design of the state matrix in the model. As a result of combining polytopic uncertainty with the controller design, the closed-loop system's robustness to uncertainties was improved when the controller was designed. After this modeling was done, a state-feedback controller was designed for the updated model to meet the H∞ criteria. By satisfying the H∞ criteria, the controller was robust to the uncertainty presented in the model. An additional result of having identified polytopic uncertainty was that it controlled the uncertainty effect on the transient matrix of systems. The advantages of this proposed approach, aside from the extremely simple structure and design, are good performance, low computational burden, good performance, and very good robustness to uncertainty while still being simple. Lastly, it effectively eliminated any chattering seen in sliding mode control families.

In the following, in Section 2, the system modeling is presented, and after presenting the mathematical relations of the desired control method in Section 3, the results of practical experiments will be presented and analyzed in Section 4. Finally, the conclusions will be expressed in the fifth section.

This paper has been accepted for publication in the AEE journal. This is the version, which has not been fully edited and content may change prior to final publication. Citation information: DOI 10.24425/aee.2026.1692

2. Dynamic equations of the servo system

Today, servo systems hold a special place in industries and are of great interest in areas such as robotics, electric vehicles, and CNC systems. The precision and speed of these systems are among engineers' most important concerns for achieving considered goals. A servo system consists of two main parts: a control board and an electric machine. The control board is responsible for generating the voltage required by the electric machine, and the electric machine provides the desired angle. One of the important types of electric machines is the permanent magnet synchronous machine, which offers high efficiency, fast response, and strong power density. This machine consists of two major parts: the rotor and the stator. The rotor contains a permanent magnet that produces a constant magnetic flux. The stator contains a three-phase winding that generates a rotating magnetic flux. Through the interaction of these two fields, the rotor begins to rotate and synchronously follows the stator's magnetic field. The dynamic behavior of the machine is expressed below [29]:

$$\begin{aligned} v_d &= L_d i_d + R i_d + n\omega_m L_q i_q, \\ v_d &= L_q i_q + R i_q + n\omega_m \left(L_d i_d + \vartheta_f\right), \\ I\ddot{\theta} &= T_e - T_L - F\omega_n, \end{aligned} \tag{1}$$

where R indicates the stator resistance; ω_m indicates the angular velocity of the rotor; θ indicates the rotor angle; L_d and L_q signify the stator inductances in the dq-axes; ϑ_f states the rotor flux linkage; i_d, i_q, v_d, and v_q refer to the stator currents and voltages in the dq-axes; n signifies the pole pairs; I signifies the moment of inertia; T_L is the load torque; F is the viscous friction constant; and T_e signifies the electromagnetic torque. For the surface-mounted servo system, T_e is derived as follows [29]:

$$T_e = 1.5 n i_q \vartheta_f. \tag{2}$$

From Eqs. (1) and (2):

$$I\ddot{\theta} = 1.5 n i_q \vartheta_f - T_L - F\omega_m. \tag{3}$$

Due to uncertainty terms caused by variations of model parameters, Eq. (3) is revised as:

$$\ddot{\theta} = 1.5 {I_n}^{-1} n i_q \vartheta_f - {I_n}^{-1} T_L - {I_n}^{-1} F_n \omega_m - {I_n}^{-1} \Delta I \ddot{\theta} - {I_n}^{-1} \Delta F \omega_m, \tag{4}$$

where I_n and F_n, respectively, are the rated values of I and F. ΔI and ΔF, respectively, are the variations of I and F. By assuming $\varepsilon = -{I_n}^{-1} T_L - {I_n}^{-1} \Delta I \ddot{\theta} - {I_n}^{-1} \Delta F \omega_m$ and $u = i_q$, there is:

$$\ddot{\theta} = 1.5 {I_n}^{-1} n \vartheta_f u - {I_n}^{-1} F_n \omega_m + \varepsilon. \tag{5}$$

By supposing θ^* as the desired angle, the angle tracking error is defined below:

$$\sigma = \theta - \theta^*. \tag{6}$$

This paper has been accepted for publication in the AEE journal. This is the version, which has not been fully edited and content may change prior to final publication. Citation information: DOI 10.24425/aee.2026.1692

From Eqs. (5) and (6), there is:

$$\ddot{\sigma} = 1.5{I_n}^{-1} n \vartheta_f u - {I_n}^{-1} F_n \omega_m + \varepsilon - \ddot{\theta}^*. \tag{7}$$

Equation (7) represents the angle tracking error dynamic for the servo system. Based on this relation, the controller design is carried out in the next section.

3. Controller design

Figure 1 presents a common structure for motor angle control based on well-established studies in the literature [29]. This structure consists of three main sections: position control, current control, and voltage conversion. According to this figure, the motor angle signal is first measured by the encoder and subtracted from the reference angle signal to obtain the angle error signal ($\boldsymbol{e_\theta}$). Then, $\boldsymbol{e_\theta}$ enters the position control section. This section is responsible for computing the reference current in the q-axis ($\boldsymbol{i_q}^*$). The current control section calculates the d- and q-axis voltages ($\boldsymbol{v_q}$ and $\boldsymbol{v_d}$) based on the measured d-q currents ($\boldsymbol{i_q}$ and $\boldsymbol{i_d}$) and their reference values ($\boldsymbol{i_q}^*$ and $\boldsymbol{i_d}^*$). Finally, the calculated d-q voltages are fed into the voltage conversion section, where the required three-phase voltages ($\boldsymbol{v_a}$, $\boldsymbol{v_b}$, and $\boldsymbol{v_c}$) for the motor are generated and the rotor follows the reference angle ($\boldsymbol{\theta}^*$). It should be noted that the voltage conversion section includes several sub-components, namely $\boldsymbol{dq/\alpha\beta}$ converter, $\boldsymbol{\alpha\beta/dq}$ converter, a PWM generator, and an inverter. It should be noted that Fig. 1 represents a common structure for motor angle control and can be implemented in various applications; it is not specific to CNC systems. This structure has been validated in reputable research articles. The implementation of this structure in CNC systems can be investigated separately in future work and is not the main focus of this paper.

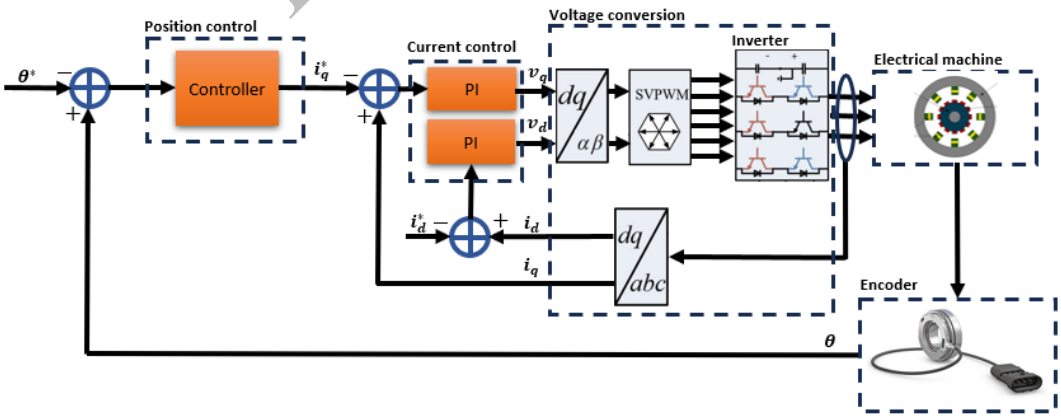

Fig. 1. The electrical board of the servo system

This paper has been accepted for publication in the AEE journal. This is the version, which has not been fully edited and content may change prior to final publication. Citation information: DOI 10.24425/aee.2026.1692

The position control section is a key section in the electrical board, and its fast, precise, and robust performance is of great importance and forms the core focus of this study.

First, based on Eq. (7) and defining $\alpha_1 = \sigma$ and $\alpha_2 = \dot{\sigma}$, there is:

$$\begin{aligned} \dot{\alpha}_1 &= \alpha_2, \\ \dot{\alpha}_2 &= 1.5{I_n}^{-1} n\vartheta_f u - {I_n}^{-1} F_n \alpha_2 + \varepsilon - {I_n}^{-1} F_n \dot{\theta}^* - \ddot{\theta}^*. \end{aligned} \tag{8}$$

The matrix form of Eq. (8) is written as follows:

$$\begin{bmatrix} \dot{\alpha}_1 \\ \dot{\alpha}_2 \end{bmatrix} = \begin{bmatrix} 0 & 1 \\ 0 & -{I_n}^{-1} F_n \end{bmatrix} \begin{bmatrix} \alpha_1 \\ \alpha_2 \end{bmatrix} + \begin{bmatrix} 0 \\ 1.5{I_n}^{-1} n\vartheta_f \end{bmatrix} u + \begin{bmatrix} 0 \\ \varepsilon \end{bmatrix} + \begin{bmatrix} 0 \\ -{I_n}^{-1} F_n \dot{\theta}^* - \ddot{\theta}^* \end{bmatrix}. \tag{9}$$

By defining $\alpha = \begin{bmatrix} \alpha_1 \\ \alpha_2 \end{bmatrix}$, $M = \begin{bmatrix} 0 & 1 \\ 0 & -{I_n}^{-1} F_n \end{bmatrix}$, $S = \begin{bmatrix} 0 \\ 1.5{I_n}^{-1} n\vartheta_f \end{bmatrix}$, $\delta = \begin{bmatrix} 0 \\ \varepsilon \end{bmatrix}$, and $E = \begin{bmatrix} 0 \\ -{I_n}^{-1} F_n \dot{\theta}^* - \ddot{\theta}^* \end{bmatrix}$, there is:

$$\dot{\alpha} = M\alpha + Su + \delta + E. \tag{10}$$

Consider that M has a polytopic form as follows:

$$M = \sum_{i=1}^{k} m_i M_i, \quad \sum_{i=1}^{k} m_i = 1, \tag{11}$$

where M_i is the i-th vertex of the polytopic region related to M, and m_i is the i-th vertex factor of the polytopic region related to M.

On the other hand, the controlled output is supposed to be:

$$y = \alpha_1. \tag{12}$$

By defining $C = [1 \quad 0]$, there is:

$$y = C\alpha. \tag{13}$$

Now, the goal is to develop a state feedback-based controller in which the effect of the uncertainty term on the angular tracking error is limited and the asymptotic stability of the closed-loop system is guaranteed. To achieve this, the H∞ criterion is introduced. Based on this criterion, if the ratio of the energy of the controlled output to the energy of the uncertainty term is bounded, the influence of the uncertainty term on the angular tracking error is bounded. Accordingly, the H∞ criterion is written as follows:

$$\frac{\int_{t=0}^{\infty} y^T y \mathrm{d}t}{\int_{t=0}^{\infty} \sigma^T \sigma \mathrm{d}t} \leq \gamma^2, \tag{14}$$

where γ^2 is the upper bound of the energy ratio.

Remark 1

Additive uncertainty is incorporated into the system model as an additive term and is characterized by an energy bound. This type of uncertainty is commonly analyzed using criteria

This paper has been accepted for publication in the AEE journal. This is the version, which has not been fully edited and content may change prior to final publication. Citation information: DOI 10.24425/aee.2026.1692

such as H_∞. For example, variations in motor parameters, noises, and environmental disturbances can be considered as additive terms added to the system model. On the other hand, in polytopic uncertainty, the system model is defined within a convex region whose bounds are determined by a set of vertices. This type of uncertainty is analyzed using LMI-based methods. For instance, the unmodeled dynamics can be described by a system model defined within a convex region. Due to $\varepsilon = -I_n^{-1}T_L - I_n^{-1}\Delta I\ddot{\theta} - I_n^{-1}\Delta F\omega_m$, considering 20% uncertainty in the moment of inertia and the viscos friction constant results in $\int_{t=0}^{\infty}\sigma^T\sigma\,\mathrm{d}t \leq 1$. Also, the vertices of polytopic region is considered as $M_1 = \begin{bmatrix}0 & 1\\ 0 & -0.8I_n^{-1}F_n\end{bmatrix}$ and $M_2 = \begin{bmatrix}0 & 1\\ 0 & -1.2I_n^{-1}F_n\end{bmatrix}$.

The control law is considered below:

$$u = K\alpha + S^{\dagger}E, \tag{15}$$

where K refers to the control gain and † refers to the pseudo-inverse symbol. By substituting Eq. (14) into Eq. (10), there is:

$$\dot{\alpha} = (M + SK)\alpha + \delta. \tag{16}$$

Referring to [30], the following stability condition ensures the H∞ criterion in Eq. (13):

$$\dot{V} \leq -y^T y + \gamma^2\delta^T\delta, \tag{17}$$

where V is a Lyapunov function defined as:

$$V = \alpha^T L\alpha. \tag{18}$$

From Eqs. (16) and (18), Eq. (17) can be extended below:

$$\begin{aligned}&\dot{\alpha}^T L\alpha + \alpha^T L\dot{\alpha} \leq -y^T y + \gamma^2\delta^T\delta \Rightarrow\\ &((M+SK)\alpha+\delta)^T L\alpha + \alpha^T L((M+SK)\alpha+\delta) \leq -y^T y + \gamma^2\delta^T\delta \Rightarrow\\ &\alpha^T(M+SK)^T L\alpha + \delta^T L\alpha + \alpha^T L(M+SK)\alpha + \alpha^T L\delta \leq -y^T y + \gamma^2\delta^T\delta.\end{aligned} \tag{19}$$

The matrix form of Eq. (19) is expressed below:

$$\begin{pmatrix}\alpha\\ \delta\end{pmatrix}^T\begin{pmatrix}(M+SK)^T L + L(M+SK) + C^T C & L\\ L^T & -\gamma^2 I\end{pmatrix}\begin{pmatrix}\alpha\\ \delta\end{pmatrix} \leq 0. \tag{20}$$

If Eq. (21) holds, then Eq. (20) holds:

$$\begin{pmatrix}(M+SK)^T L + L(M+SK) + C^T C & L\\ L^T & -\gamma^2 I\end{pmatrix} \leq 0. \tag{21}$$

Supposing $W = LSK$, Eq. (21) can be written below:

$$\begin{pmatrix}M^T L + W^T + LM + W + C^T C & L\\ * & -\gamma^2 I\end{pmatrix} \leq 0. \tag{22}$$

This paper has been accepted for publication in the AEE journal. This is the version, which has not been fully edited and content may change prior to final publication. Citation information: DOI 10.24425/aee.2026.1692

Since the polytopic forms in Eq. (11) have the convex property, if Eq. (23) holds, then Eq. (22) holds:

$$\begin{pmatrix} {M_i}^T L + W^T + L M_i + W + C^T C & L \\ * & -\gamma^2 I \end{pmatrix} \leq 0, \quad i = 1, \ldots, k. \tag{23}$$

Now, based on Eq. (23), the following optimization problem is presented to reach the best performance:

$$\begin{gathered} \min \gamma \\ \text{subject to:} \\ \begin{pmatrix} {M_i}^T L + W^T + L M_i + W + C^T C & L \\ * & -\gamma^2 I \end{pmatrix} \leq 0, \quad i = 1, \ldots, k \end{gathered}. \tag{24}$$

Equation (24) has a linear matrix inequality (LMI) form. Therefore, solving Eq. (24) using the YALMIP toolbox in MATLAB, the parameters L, W, and γ are derived. Consequently, K is calculated below:

$$K = (LS)^{\dagger} W. \tag{25}$$

Finally, u is calculated as follows:

$$u = (LS)^{\dagger} W \alpha + S^{\dagger} E. \tag{26}$$

Remark 2

In this study, we use the H_∞ criterion in Eq. (14). Equation (14) expresses that the ratio of the output energy y to the energy of the additive uncertainty σ should be less than γ^2. The smaller the value of γ^2, the less the effect of the additive uncertainty on the output. As proven in [30], the stability condition in Eq. (17) guarantees the H_∞ criterion in Eq. (14). Therefore, Eq. (17) represents a robust stability condition. On the other hand, the control law u is considered as a state-feedback form in Eq. (15). Now, we intend to extract the control gain K in a such way that Eq. (17) is satisfied. Accordingly, an attempt has been made to convert Eq. (17) into an LMI inequality given in Eq. (22) based on Eq. (15). Now, in order to achieve maximum robustness against the additive uncertainty, the optimization problem in Eq. (24) is formulated to obtain the minimum value of γ^2 for which Eq. (22) is feasible. This value depends on the values of the state-space matrices M and S, which are determined through experimental test on a sample motor. It should be noted that the H_∞ criterion attempts to minimize the effect of the uncertainty energy, with limited bound, on the output energy. With γ^2 assumed to be constant and according to Eq. (14), as the uncertainty energy increases, the output energy also increases, and the tracking performance deteriorates.

In experimental test, Eq. (24) is first solved offline to obtain K. Subsequently, Eq. (15) is implemented on microprocessor to calculate control law u.

The feasibility region in the optimization problem in Eq. (24) is defined as $\gamma \geq r$. The value of r can be obtained based on the values of motor parameter in experimental tests.

This paper has been accepted for publication in the AEE journal. This is the version, which has not been fully edited and content may change prior to final publication. Citation information: DOI 10.24425/aee.2026.1692

It is acknowledged that a full industrial motion control system comprises more than a single position loop; elements such as function generators with multiple operating modes, interpolators, cascaded speed and current loops, and various signal conditioning filters (PT1 low-pass, PT2 low-pass, general second-order, and band-stop notch filters) are typically integrated to handle periodic and non-periodic reference signals. However, the primary contribution of this paper is not to propose a complete drive architecture but rather to introduce a robust H∞ state feedback controller for the outer position loop, which is the most critical layer for angular tracking accuracy under summative and polytopic uncertainties. The proposed controller generates the *q*-axis current reference, which serves as the input to the inner current loops. The missing modules—such as reference signal generators with different waveforms, pre-filters, and disturbance feedforward paths—are orthogonal to our design and can be added as pre-processing or post-processing stages without affecting the stability or H∞ performance guarantees established in this work. Therefore, the proposed method is compatible with more complex industrial structures and can be seamlessly integrated into existing servo drives that utilize such filters and function generator modes.

4. Practical tests and analysis

In this section, the results of practical experiments designed to measure the performance of the control method will be presented and analyzed. In these experiments, a laboratory accelerator shown in Fig. 2(a) was used, and all the functions of the proposed method were simulated with the performance of the adaptive sliding mode control (ASMC) method.

The proposed H∞ state feedback controller generates the *q*-axis current reference, which directly corresponds to the "current setpoint after the filter" operating mode of the function generator in a standard servo drive. This signal can be routed through the signal conditioning block (including PT1 low-pass, PT2 low-pass, second-order general, or notch filters) before entering the vector controller. Alternatively, the controller output can be configured as the "current setpoint before the filter" if additional filtering is desired within the drive. While the proposed method does not explicitly utilize speed setpoint modes or disturbing torque feedforward, the modular structure of the function generator allows seamless integration without modifying the existing industrial architecture. Therefore, the simplicity of the proposed controller does not compromise compatibility with advanced motion control systems.

The PMSM motor involved in the experiment was a six-pole surface-mounted machine, modeled as the FAPMSM-240-6. The PMSM was connected to a three-phase IGBT bridge (the PrimePower IGBT-450V4QS), providing the drive signals. A servo driver, the DynaDrive-SV-300, controlled the motor currents in accordance with the vector control algorithm. Real-time rotor position and speed information was obtained via a torque/position sensor package called the SensoTorque TPS-120. Electrical measurements and motor parameters were recorded using a National Instruments PCIe-6351 data acquisition (DAQ) card, which sampled current, voltage, and rotor position at a rate of 20 kS/s. The acquisition was

This paper has been accepted for publication in the AEE journal. This is the version, which has not been fully edited and content may change prior to final publication. Citation information: DOI 10.24425/aee.2026.1692

synchronized via a hardware clock. A lab power supply powered the DAQ and controller electronics, the HP-330W DC supply, with the supplied comfortable high-frequency DC-link capacitor bank, the Nichicon UHP 6 800 μF, 450 V. An experimental rig was constructed from a motor mount (Albright Power Electronics), a torque transducer (Omega TQ-202), and a cooling assembly to allow thermal stability during testing.

On this experimental tests' setup, the proposed controller and also the ASMC controller were implemented to be compared to each other. The algorithm of the proposed controller has been expressed in Section 2.

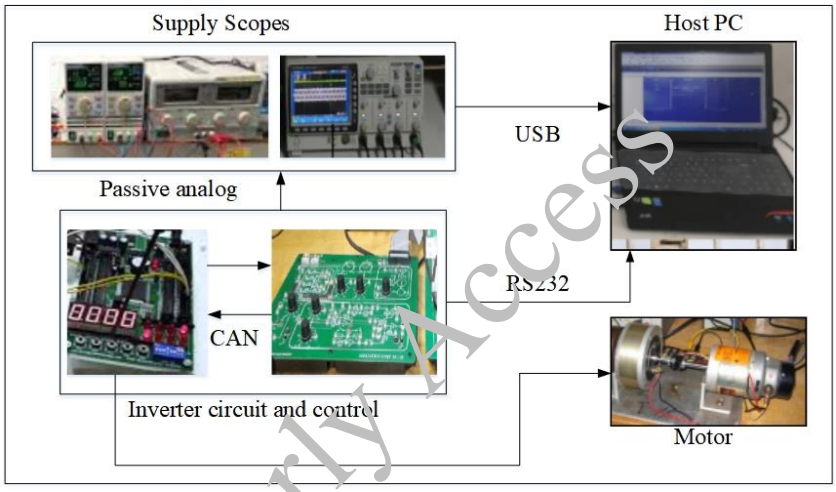

(a)

This paper has been accepted for publication in the AEE journal. This is the version, which has not been fully edited and content may change prior to final publication. Citation information: DOI 10.24425/aee.2026.1692

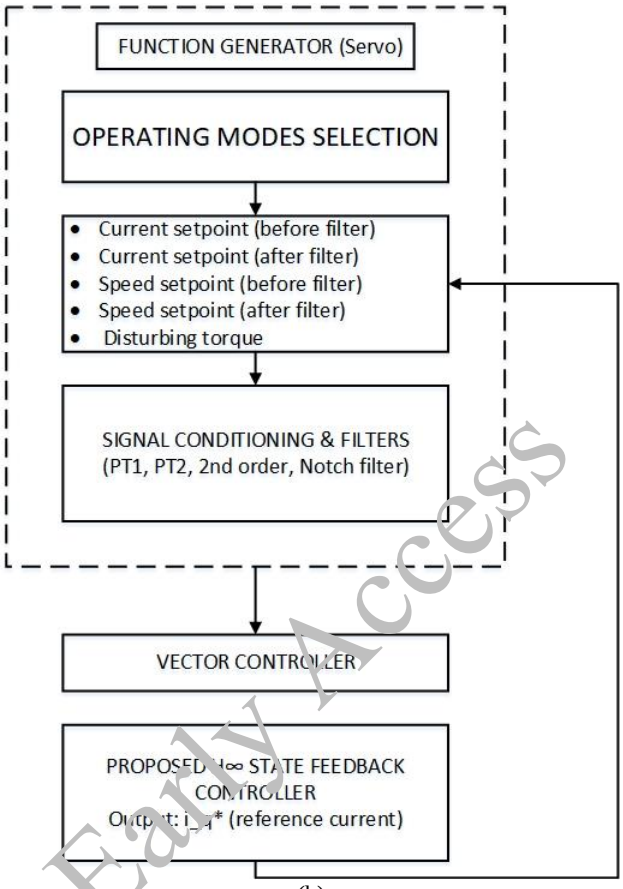

(b)

Fig. 2. Test setup (a); operating modes of the function generator in the servo motion control system and the integration point of the proposed H∞ state feedback controller (b)

The ASMC for PMSM servo angle control combines the robustness of sliding-mode control with online parameter adaptation to cope with model uncertainties such as load torque variations, resistance changes, and unmodeled dynamics. The controller defines a tracking-error-based sliding surface and injects a switching term to enforce finite-time convergence, while an adaptive law adjusts uncertain parameters in real-time to reduce chattering and improve steady-state precision. This structure ensures high tracking accuracy, strong disturbance rejection, and stable performance across a wide operating range.

Design parameters of the ASMC are reported in Table 1.

This paper has been accepted for publication in the AEE journal. This is the version, which has not been fully edited and content may change prior to final publication. Citation information: DOI 10.24425/aee.2026.1692

Table 1. Design parameters of the ASMC

Parameter	Value
Proportional gain of sliding surface	60
Derivative gain (if used)	4
Sliding surface slope	120
Switching (reaching law) gain	14
Boundary layer thickness (for saturation function)	0.01–0.05 rad
Adaptation gain for parameter update	84

Table 2. Motor specs

Rated power	3
Frequency	50
Rated speed	1 000
Rated torque	10
Poles	6
Efficiency	85

In the first phase of practical experiments, the performance of the desired control method is tested in a steady state. In this case, the best possible scenario is to select the control loop input as a reference for the motor angle as a step signal. But to make things a little more complicated in these experiments, a step signal that has been increased in two stages is added to the control loop. The results of these experiments are shown in Fig. 3, and as is clear, the reference angle first reaches 2 radians and then 4 radians. The performance results of the control method considered in this article and the SMC method are compared with each other in this figure and Fig. 4. According to this figure, it is quite evident that the proposed method has a lower convergence speed, higher steady-state accuracy, and less chattering phenomenon. More precisely, the proposed method was able to converge to the reference value within 0.1 seconds and had a steady-state error of 0.1 radian. On the other hand, it is quite obvious that the proposed method has less overshoot when making changes to the reference angle. But in contrast, it is quite evident that the ASMC method has a convergence time of 0.3 seconds and a steady-state error of 0.22 radians. In addition to higher transmutation in the ASMC method, the chattering phenomenon is also higher, which indicates that the method in question was more successful in reducing the chattering phenomenon. Figure 5 shows the control signal generated by the

This paper has been accepted for publication in the AEE journal. This is the version, which has not been fully edited and content may change prior to final publication. Citation information: DOI 10.24425/aee.2026.1692

controller for this input, and the values obtained indicate the feasibility of the desired method. Below this amount, the produced values are not outside the motor's tolerable limits.

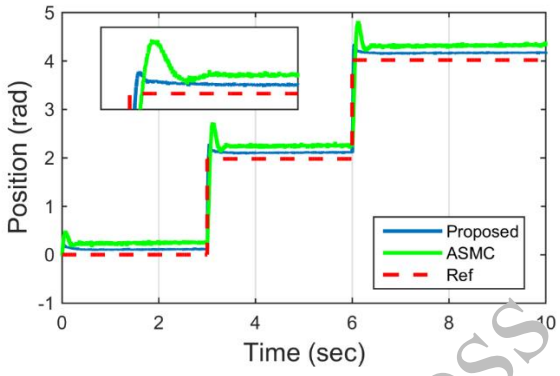

Fig. 3. Step tracking scenario

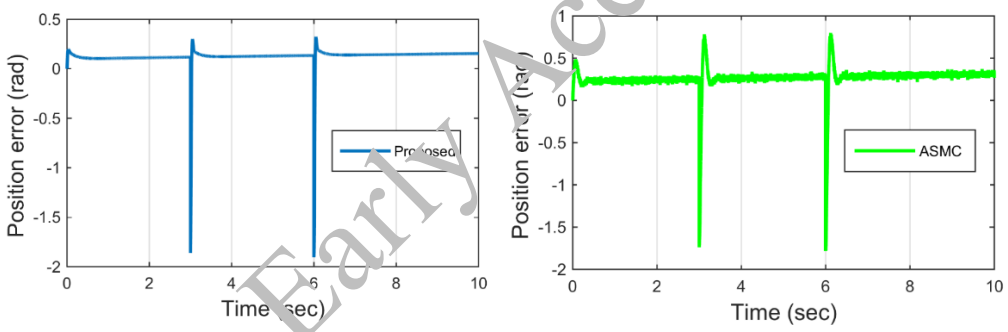

(a) (b)

Fig. 4. Step tracking error: propsed mehod (a); ASMC (b)

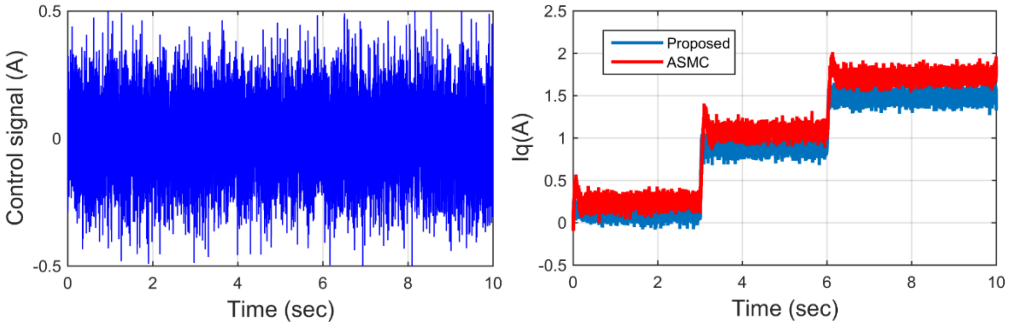

Fig. 5. Motor current and control signal in the step scenario

This paper has been accepted for publication in the AEE journal. This is the version, which has not been fully edited and content may change prior to final publication. Citation information: DOI 10.24425/aee.2026.1692

In the second phase of practical tests, the purpose was to measure the performance of control methods in accelerated or transient modes. Therefore, the control loop input is considered as a ramp signal that has different accelerations during ascent and descent. The results of this scenario are shown in Figs. 6 and 7, and as can be seen from this figure, the motor first reaches approximately 2 radians within one second and then returns to zero after 2 seconds. According to this figure and Fig. 7, which shows the tracking error, it is quite clear that the proposed method still performs better. In other words, the proposed method was able to track the reference input with a steady-state error of 0.15 radians. But on the other hand, the ASMC method has a steady-state error of 0.35 radians, which indicates that due to the lower convergence speed, the motor angle has always lagged behind the reference angle, causing a bias and error. On the other hand, the presence of more chatter in the performance of the ASMC method indicates that the method in question was more successful in reducing this phenomenon. In Fig. 8, the control signal generated in this scenario is also plotted, and as is clear, even in accelerated moments, the controller was able to generate a reasonable signal and not exceed the motor limits.

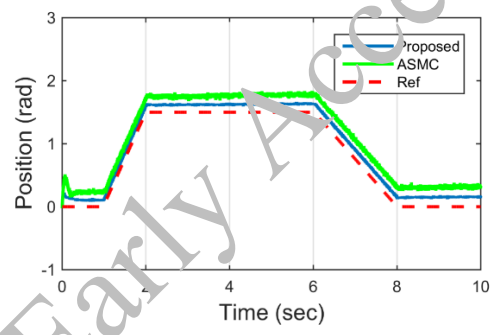

Fig. 6. Reference tracking in transient mode

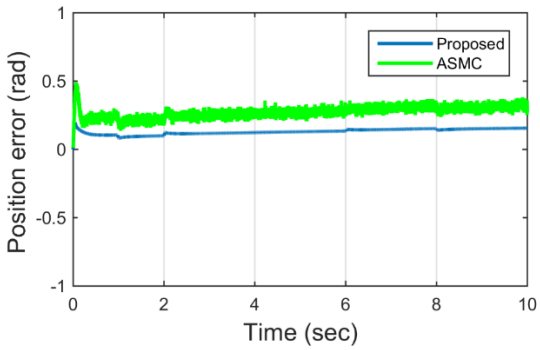

Fig. 7. Tracking error in transient mode

This paper has been accepted for publication in the AEE journal. This is the version, which has not been fully edited and content may change prior to final publication. Citation information: DOI 10.24425/aee.2026.1692

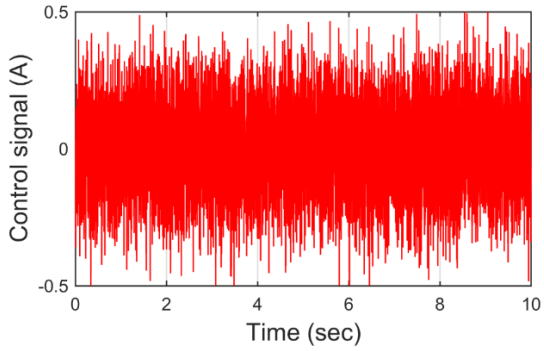

Fig. 8. Control signal generated in transient scenario

In the third phase of practical tests, the performance of the proposed method is validated under the load variation, measurement noise, and parameter changes. To be more specific, at time 6s, the load on the motor shat changes as much as 10%. In addition, the model parameters of the motor have been changed as much as 10% to make a difference between the model used for the control design and the actual model of the motor. The results of this experiment are shown in Figs. 9 and 10. As is clear from these figures, the load variation causes a jump in the performance of both control methods. But, the proposed method returns the position to the reference value in a shorter time and with lower jump. Moreover, the proposed controller has the tracking error of 0.11 rad and has the convergence time of 0.095 s. On the other hand, the ASMC has the tracking error of 0.3 rad with the convergence time of 0.35 s. This scenario confirms that in the presence of parameter variations, load variation, and disturbances, the proposed method is a more reliable choice. In Table 2 a quantitative comparison between methods with more comparison metrics is reported.

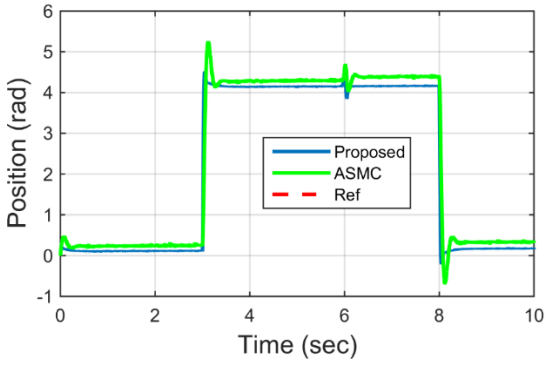

Fig. 9. Reference tracking in load and parameter variation

This paper has been accepted for publication in the AEE journal. This is the version, which has not been fully edited and content may change prior to final publication. Citation information: DOI 10.24425/aee.2026.1692

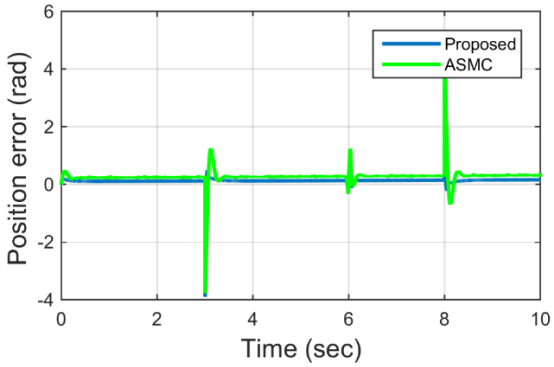

Fig. 10. Tracking error in in load and parameter variation

Table 3. Quantitative comparison

Method and scenario		Tracking error (rad)	Convergence time (s)	Overshoot (rad)	Control energy	H∞ norm value	Settling time (s)	RMSE (rad)	Control effort variance
SC 1	Proposed	0.1	0.1	0.08			0.1	0.08	
	ASMC	0.22	0.3	0.4			0.3	0.18	
SC 2	Proposed	0.15	0.1	0.02			0.1	0.12	
	ASMC	0.35	0.32	0.09			0.32	0.30	
SC 3	Proposed	0.11	0.095	0.08			0.095	0.09	
	ASMC	0.3	0.35	0.4			0.35	0.22	

Regarding the operating speed range, this study focuses on the low-to-moderate speed region (0–1 000 rpm), which is the most critical zone for high-precision position tracking in CNC machining, robotic manipulation, and industrial servo positioning, where friction, cogging torque, and load disturbances have the most pronounced effects. Tests at very high speeds (above rated speed) are intentionally deferred to future work, as they introduce dominant back-EMF and voltage saturation effects that require additional field-weakening considerations. The feedback type employed is incremental encoder-based position feedback (20 000 pulses per revolution) combined with numerical differentiation for velocity estimation, forming a standard cascade structure with position loop outer and current loop inner. Furthermore, in the context of motion control systems with a position controller and motion interpolator, the proposed H∞ state feedback controller operates at the position-loop level, receiving the reference angle from the trajectory generator. The function generator in a commercial servo drive typically provides several output modes—such as current setpoint before/after the filter, speed setpoint before/after

This paper has been accepted for publication in the AEE journal. This is the version, which has not been fully edited and content may change prior to final publication. Citation information: DOI 10.24425/aee.2026.1692

the filter, and disturbing torque—which are essential for implementing nested control loops. While these modules are not the focus of this paper, they are fully compatible with our design: the output of our H∞ controller serves as the *q*-axis current reference, which can be directly fed into the vector control's current setpoint input after the filter, preserving the standard industrial architecture. Thus, the simplicity and robustness of the proposed method do not preclude integration with more complex motion control structures involving interpolators and multi-mode function generators.

5. Conclusion

This study has focused on robustness against model uncertainties and simplicity in controller design for position control in servo systems. The permanent magnet synchronous motor was modeled with uncertainties included as a sum term of the state space equations, and to increase robustness, a polytopic uncertainty was introduced in the design of the state matrix. After the controller is designed, this combination creates a closed-loop system that is resistant to uncertainties. Following this, a state-feedback controller was implemented with the new model for the explicit purpose of satisfying the H∞ criterion imposed by the task. This will also create performance guarantees of robustness to cumulative model uncertainties. This also resulted in some measure of robustness to variations in the transient matrix when including polytopic uncertainties. One of the main benefits identified is the exceptionally simple structure and design that equates to a low computational load while offering a strong level of robustness. Furthermore, the approach successfully reduced the chattering effects associated with sliding mode control families. To evaluate this approach, an extensive set of laboratory experiments was conducted to demonstrate this approach's validity in the ten circumstances modeled. The work presented in this work demonstrates that an incredibly modest yet rigorous design can yield robust performance against both transience and model uncertainties without excessive computational costs.

References

[1] Zhao Y., Wei C., Zhang Z., Qiao W., *A review on position/speed sensorless control for permanent-magnet synchronous machine-based wind energy conversion systems*, IEEE J. Emerg. Sel. Top. Power Electron., vol. 1, no. 4, pp. 203–216 (2013), DOI: 10.1109/JESTPE.2013.2280572.

[2] Li Y., Wu H., Xu X., Sun X., Zhao J., *Rotor position estimation approaches for sensorless control of permanent magnet traction motor in electric vehicles: A review*, World Electric Vehicle Journal, vol. 12, no. 1, 9 (2021), DOI: 10.3390/wevj12010009.

[3] Khubalkar S., Junghare A., Aware M., Das S., *Modeling and control of a permanent-magnet brushless DC motor drive using a fractional order proportional-integral-derivative controller*, Turkish Journal of Electrical Engineering and Computer Sciences, vol. 25, no. 5, pp. 4223–4241 (2017), DOI: 10.3906/elk-1612-277.

This paper has been accepted for publication in the AEE journal. This is the version, which has not been fully edited and content may change prior to final publication. Citation information: DOI 10.24425/aee.2026.1692

[4] Lin F.-J., *Real-time IP position controller design with torque feedforward control for PM synchronous motor*, IEEE Transactions on industrial electronics, vol. 44, no. 3, pp. 398−407 (1997), DOI: 10.1109/41.585839.
[5] Tarczewski T., Grzesiak L.M., *High precision permanent magnet synchronous servo-drive with lqr position controller*, Electrical Review, vol. 85, no. 8, pp. 42–47 (2009).
[6] Wang Y., Liu X., *Model predictive position control of permanent magnet synchronous motor servo system with sliding mode observer*, Asian J. Control, vol. 25, no. 1, pp. 443−461 (2023), DOI: 10.1002/asjc.2817.
[7] Wei Y., Wei Y., Sun Y., Qi H., Guo X., *Prediction horizons optimized nonlinear predictive control for permanent magnet synchronous motor position system*, IEEE Transactions on Industrial Electronics, vol. 67, no. 11, pp. 9153–9163 (2019).
[8] Mubarok M.S., Liu T.-H., *Implementation of predictive controllers for matrix-converter-based interior permanent magnet synchronous motor position control systems*, IEEE J. Emerg. Sel. Top. Power Electron., vol. 7, no. 1, pp. 261–273 (2018), DOI: 10.1109/JESTPE.2018.2873151.
[9] Dhaouadi R., Mohan N., Norum L., *Design and implementation of an extended Kalman filter for the state estimation of a permanent magnet synchronous motor*, IEEE Trans. Power Electron., vol. 6, no. 3, pp. 491–497 (1991), DOI: 10.1109/63.85891.
[10] Qiao Z., Shi T., Wang Y., Yan Y., Xia C., He X., *New sliding-mode observer for position sensorless control of permanent-magnet synchronous motor*, IEEE Transactions on Industrial electronics, vol. 60, no. 2, pp. 710–719 (2012), DOI: 10.1109/TIE.2012.2186779.
[11] Liu Y.-C., *Disturbance-observer-based second-order sliding-mode position control for permanent-magnet synchronous motors: a continuous twisting algorithm-based approach*, Energies (Basel), vol. 17, no. 12, 2974 (2024), DOI: 10.3390/en17122974.
[12] Zhao Y., Zhang Z., Qiao W., Wu L., *An extended flux model-based rotor position estimator for sensorless control of salient-pole permanent-magnet synchronous machines*, IEEE Trans. Power Electron., vol. 30, no. 8, pp. 4412–4422 (2014), DOI: 10.1109/TPEL.2014.2358021.
[13] Senhaji A., Abdelouhab M., Attar A., Bouchnaif J., *Backstepping control of a permanent magnet synchronous motor*, Mater. Today Proc., vol. 72, pp. 3730–3737 (2023), DOI: 10.1016/j.matpr.2022.09.248.
[14] Wang H., Liu X., *Permanent magnet synchronous motor feedback linearization vector control*, Mechatronics and Automatic Control Systems: Proceedings of the 2013 International Conference on Mechatronics and Automatic Control Systems (ICMS2013), Springer, pp. 601–608 (2013).
[15] Morawiec M., *The adaptive backstepping control of permanent magnet synchronous motor supplied by current source inverter*, IEEE Trans. Industr. Inform., vol. 9, no. 2, pp. 1047−1055 (2012), DOI: 10.1109/TII.2012.2211327.
[16] Hans S., Ghosh S., *Position analysis of brushless direct current motor using robust fixed order H-infinity controller*, Assembly Automation, vol. 40, no. 2, pp. 211–218 (2020).
[17] . Jung T.-U., Jang J.-H., Park C.-S., *A back-EMF estimation error compensation method for accurate rotor position estimation of surface mounted permanent magnet synchronous motors*, Energies (Basel), vol. 10, no. 8, 1160 (2017), DOI: 10.3390/en10081160.
[18] Zhao Z., Hu C., Wang Z., Wu S., Liu Z., Zhu Y., *Back EMF-based dynamic position estimation in the whole speed range for precision sensorless control of PMLSM*, IEEE Trans. Industr. Inform., vol. 19, no. 5, pp. 6525–6536 (2022).
[19] Lu H., Yang D., Su Z., *Improved sliding mode control for permanent magnet synchronous motor servo system*, IET Power Electronics, vol. 16, no. 2, pp. 169–179 (2023).
[20] Namuduri C., Sen P.C., *A servo-control system using a self-controlled synchronous motor (SCSM) with sliding mode controller*, IEEE Trans. Ind. Appl., no. 2, pp. 283–295 (2008).

This paper has been accepted for publication in the AEE journal. This is the version, which has not been fully edited and content may change prior to final publication. Citation information: DOI 10.24425/aee.2026.1692

[21] Wai R.-J., *Total sliding-mode controller for PM synchronous servo motor drive using recurrent fuzzy neural network*, IEEE Transactions on Industrial Electronics, vol. 48, no. 5, pp. 926–944 (2001), DOI: 10.1109/41.954557.

[22] Sun X., Cao J., Lei G., Guo Y., Zhu J., *Speed sensorless control for permanent magnet synchronous motors based on finite position set*, IEEE Transactions on Industrial Electronics, vol. 67, no. 7, pp. 6089–6100 (2019), DOI: 10.1109/TIE.2019.2947875.

[23] Bobtsov A.A., Pyrkin A.A., Ortega R., Vukosavic S.N., Stankovic A.M., Panteley E.V, *A robust globally convergent position observer for the permanent magnet synchronous motor*, Automatica, vol. 61, pp. 47–54 (2015), DOI: 10.1016/j.automatica.2015.06.009.

[24] Wei Y., Wei Y., Sun Y., Qi H., Guo X., *Prediction horizons optimized nonlinear predictive control for permanent magnet synchronous motor position system*, IEEE Transactions on Industrial Electronics, vol. 67, no. 11, pp. 9153–9163 (2019).

[25] Wei Y., Wei Y., Sun Y., Qi H., Guo X., *Prediction horizons optimized nonlinear predictive control for permanent magnet synchronous motor position system*, IEEE Transactions on Industrial Electronics, vol. 67, no. 11, pp. 9153–9163 (2019).

[26] Peng W.-L., Lan Y.-W., Chen S.-G., Lin F.-J., Chang K.-L., Ho J.-M., *Reinforcement learning control for six-phase permanent magnet synchronous motor position servo drive*, 2020 3rd IEEE International Conference on Knowledge Innovation and Invention (ICKII), IEEE, pp. 332–335 (2020).

[27] Zhu W., Chen D., Du H., Wang X., *Position control for permanent magnet synchronous motor based on neural network and terminal sliding mode control*, Transactions of the Institute of Measurement and Control, vol. 42, no. 9, pp. 1632–1640 (2020), DOI: 10.1177/0142331219893799.

[28] Bui M.X., Dutta R., Rahman F., *Application of deep learning in parameter estimation of permanent magnet synchronous machines*, IEEE Access, vol. 12, pp. 40710–40721 (2024), DOI: 10.1109/ACCESS.2024.3377224.

[29] Shi J.-L., Liu T.-H., Chang Y.-C., *Position control of an interior permanent-magnet synchronous motor without using a shaft position sensor*, IEEE Transactions on Industrial Electronics, vol. 54, no. 4, pp. 1989–2000 (2007), DOI: 10.1109/TIE.2007.895137.

[30] Lee S.-M., Park J.H., *Robust H∞ model predictive control for uncertain systems using relaxation matrices*, Int. J. Control, vol. 81, no. 4, pp. 641–650 (2008), DOI: 10.1080/00207170701579411.